Two distinct anionic phospholipid-dependent events involved in SecA-mediated protein translocation

Koch, Sabrina; Exterkate, Marten; López, Cesar A; Patro, Megha; Marrink, Siewert J; Driessen, Arnold J M

Published in:
Biochimica et Biophysica Acta - Biomembranes

DOI:
10.1016/j.bbamem.2019.183035

Publication date:
2019

BBA - Biomembranes 1861 (2019) 183035

Contents lists available at ScienceDirect

BBA - Biomembranes

journal homepage: www.elsevier.com/locate/bbamem

Two distinct anionic phospholipid-dependent events involved in SecA-mediated protein translocation

Sabrina Koch[a,1], Marten Exterkate[a,1], Cesar A. López[b,c,1], Megha Patro[a], Siewert J. Marrink[b], Arnold J.M. Driessen[a,*]

[a] Department of Molecular Microbiology, Groningen Biomolecular Sciences and Biotechnology Institute and Zernike Institute for Advanced Materials, University of Groningen, Nijenborgh 7, 9747 AG Groningen, the Netherlands
[b] Department of Molecular Dynamics, Groningen Biomolecular Sciences and Biotechnology Institute and Zernike Institute for Advanced Materials, University of Groningen, Nijenborgh 7, 9747 AG Groningen, the Netherlands
[c] Theoretical Biology and Biophysics Group, Los Alamos National Laboratory, NM, USA

ARTICLE INFO

Keywords:
Nanodiscs
SecYEG
Protein-lipid interactions
Protein translocation
Anionic phospholipids
Molecular dynamics

ABSTRACT

Protein translocation across the bacterial cytoplasmic membrane is an essential process catalyzed by the Sec translocase, which in its minimal form consists of the protein-conducting channel SecYEG, and the motor ATPase SecA. SecA binds *via* its positively charged N-terminus to membranes containing anionic phospholipids, leading to a lipid-bound intermediate. This interaction induces a conformational change in SecA, resulting in a high-affinity association with SecYEG, which initiates protein translocation. Here, we examined the effect of anionic lipids on the SecA-SecYEG interaction in more detail, and discovered a second, yet unknown, anionic lipid-dependent event that stimulates protein translocation. Based on molecular dynamics simulations we identified an anionic lipid-enriched region in vicinity of the lateral gate of SecY. Here, the anionic lipid headgroup accesses the lateral gate, thereby stabilizing the pre-open state of the channel. The simulations suggest flip-flop movement of phospholipid along the lateral gate. Electrostatic contribution of the anionic phospholipids at the lateral gate may directly stabilize positively charged residues of the signal sequence of an incoming preprotein. Such a mechanism allows for the correct positioning of the entrant peptide, thereby providing a long-sought explanation for the role of anionic lipids in signal sequence folding during protein translocation.

1. Introduction

About 25–30% of bacterial proteins carry out their metabolic and structural function outside the cytoplasm. Therefore, they either have to be inserted into, or translocated across the cytoplasmic membrane. The major route for membrane protein insertion and translocation in bacteria is provided by the secretory (Sec) pathway. Targeting of proteins to the Sec translocase occurs either post-translationally *via* an amino-terminal (N-terminal) signal sequence or co-translationally as ribosome nascent chains with the aid of signal recognition particles (SRP) [1]. During post-translational targeting, the hydrophobic core of a preprotein is recognised and bound by the molecular chaperone SecB, keeping the preprotein in an unfolded, secretion-competent state. The SecB-preprotein complex is then targeted to the motor ATPase SecA [2], which is bound to the membrane-embedded protein-conducting channel SecYEG and translocation is initiated.

The SecYEG complex comprises a heterotrimeric organization of three integral membrane proteins SecY, SecE and SecG [3]. SecY consists of 10 α-helical transmembrane helices (TMH) and is divided into an N-terminal (TMH 1–5) and C-terminal domain (TMH 6–10), which are connected by a periplasmic loop forming a clamshell structure with a centrally located pore. The pore ring, which is composed of hydrophobic residues, separates the periplasmic and cytoplasmic hydrophilic environments on both sides of the membrane. The channel is plugged

Abbreviations: N-terminal, amino-terminal; IPTG, isopropyl 1-thio-β-D-galactopyranoside; OmpA, outer membrane protein A; DDM, n-Dodecyl β-D-maltoside; Apo, apolipoprotein; PC, phosphatidylcholine; PG, phosphatidylglycerol; PE, phosphatidylethanolamine; PS, phosphatidylserine; CL, cardiolipin; PA, phosphatidic acid; MD, molecular dynamics; CG, coarse-grained; AA, all-atom; MST, Microscale Thermophoresis; LC-MS, Liquid Chromatography - Mass Spectrometry; SRP, signal recognition particles; TMH, transmembrane helix; SMA, styrene maleic acid

* Corresponding author.
E-mail addresses: s.koch@rug.nl (S. Koch), m.exterkate@rug.nl (M. Exterkate), cesar@lanl.gov (C.A. López), megha.patro@sgbm.uni-freiburg.de (M. Patro), s.j.marrink@rug.nl (S.J. Marrink), a.j.m.driessen@rug.nl (A.J.M. Driessen).
[1] Authors contribute equally.

https://doi.org/10.1016/j.bbamem.2019.183035
Received 11 February 2019; Received in revised form 30 July 2019; Accepted 1 August 2019
Available online 05 August 2019

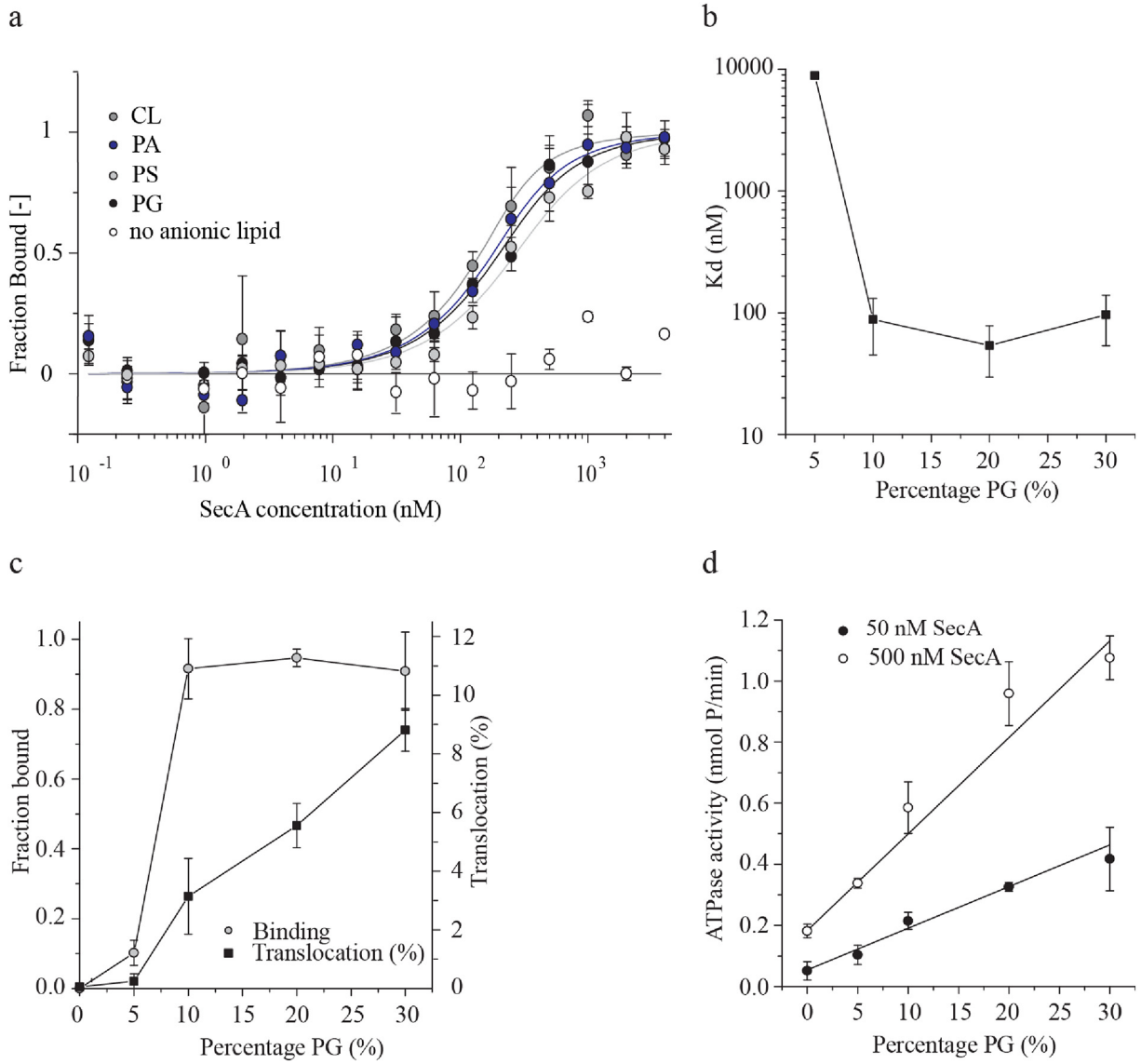

Fig. 1. Anionic lipid concentration dependency of the SecA-SecYEG interaction, translocation activity and ATPase activity. (a) Microscale Thermophoresis (MST) analysis of the binding of SecA to SecYEG reconstituted in nanodiscs harboring either CL (dark grey), PA (blue), PS (light grey), PG (black) or no anionic lipid (white). Fraction of bound SecYEG was plotted as a function of the SecA concentration. (b) Anionic lipid concentration dependent SecA-SecYEG binding. The apparent K_D values were determined by MST and plotted against the corresponding PG percentage present in the SecYEG nanodiscs. (c) The anionic lipid concentration dependent SecA-SecYEG binding and translocation activity. The fraction of bound SecYEG nanodiscs, was determined at a SecA concentration of 1000 nM by MST (left y-axis), and plotted against the percentage of PG in the membrane (open symbols). Translocation activity was tested by SecA-dependent translocation of proOmpA into SecYEG proteoliposomes. The percentage of translocated proOmpA at a SecA concentration of 1000 nM (right y-axis) was plotted against the PG percentage present in the membrane (filled symbols). (d) Anionic lipid concentration dependent ATPase activity of SecA during translocation of proOmpA into SecYEG proteoliposomes. ATPase activity was measured in the presence of 50 nM (filled symbols) and 500 nM (open symbols) SecA, and the data points were fitted linear using the equation $y = a + bx$.

on the periplasmic side by a short helix (TMH2a) in the centre of SecY, and a loosened junction between TMH2b and TMH7 of SecY forms a lipid-facing lateral gate [4]. When SecA interacts with the preprotein and SecYEG, it is activated for the ATP-dependent stepwise translocation of preproteins [5,6]. In the initial stages of the process, the N-terminal signal sequence of the preprotein binds at a site close to the lateral gate, whereupon it intercalates into the lateral gate [7], and eventually slides outside of the lateral gate [8]. It was proposed that the signal sequence relocates in such a way that the N-terminus is located towards the cytoplasm, while the C-terminus is oriented towards the periplasm [8,9]. The positioning of the signal sequence in the lateral gate leads to a widening of the pore ring, which in turn causes the plug to shift outwards. This mechanism results in the formation of a central channel that can accommodate a translocating polypeptide. The pore ring acts as a gasket surrounding the polypeptide, thereby preventing any undesired ion leaks [8].

The numerous components and their interplay demonstrate the complexity of translocation, in which not only proteins, but also the phospholipid membrane plays a crucial role. The lipid bilayer provides a matrix in which the Sec-channel is embedded, allowing for specific translocon-phospholipid interactions. In particular anionic lipids have been shown to interact with SecYEG [10] and are essential for protein translocation [11,12], while other lipids species, like the zwitterionic non-bilayer lipid phosphatidylethanolamine (PE) have a stimulating effect on the translocation process [13]. Recently, we have shown that anionic phospholipids are needed for the high affinity binding of SecA to SecYEG. In this process, SecA binds to anionic lipids (*e.g.* phosphatidylglycerol) in the cytoplasmic membrane *via* its amphipathic

positively charged N-terminus [14]. This enables the tethering of SecA to the membrane [15] and allosterically alters the SecA conformation, thereby promoting its binding to SecYEG with high affinity [14] and stimulating its ATPase activity for protein translocation [12].

Although these findings provide a first mechanistic insight into how anionic lipids participate in protein translocation, still little is known about the specific influence of the anionic lipids on the SecA-SecYEG interaction. Here, we further elaborated on the anionic phospholipid dependent binding of SecA to the translocon by combining experimental data with molecular dynamics simulations, to provide a more detailed insight on how anionic lipids influence post-translational protein translocation.

2. Results

2.1. Anionic phospholipid dependence of protein translocation and SecA-SecYEG binding

One of the bacterial translocation related processes in which anionic lipids function is the interaction of SecA with the translocon. Recently, it was shown that phosphatidylglycerol (PG), one of the major lipid species in *E. coli*, is needed for the high affinity binding of SecA to the SecYEG channel [14]. In this process, SecA initially associates with the membrane *via* a weak interaction of the SecA N-terminal amphipathic helix with PG, which induces a conformational change in SecA that enables subsequent high-affinity binding to the SecYEG channel. Given that the nature of the SecA N-terminus PG interaction is electrostatic [16], the binding mechanism of SecA to the membrane may not be specifically mediated by PG, but might be realized with other anionic lipid species as well [14]. To verify the charge-dependency of this interaction, we investigated the influence of the anionic lipid species phosphatidylserine (PS), phosphatidic acid (PA) and cardiolipin (CL), and compared it with PG. Single SecYEG complexes were reconstituted into large nanodiscs (size ~31 nm) as SecA needs a large lipid surface in order to be able to penetrate the lipid bilayer with its N-terminus [14]. The nanodiscs were prepared with a lipid composition of anionic lipid:PE:PC (molar ratio 30:30:40), except for CL, which contains an additional negative charge. As the effect of charge is examined, the molar ratio was adjusted to CL:PE:PC 15:30:40 to keep the overall net charge constant. SecA-SecYEG binding was assessed by Microscale Thermophoresis (MST). Reconstituted SecYEG was fluorescently labelled with Cy5 at a unique Cys 148 position of SecY and a binding curve was obtained by titration with SecA. Regardless of the anionic lipid type, SecA binding to the SecYEG containing nanodiscs followed a similar pattern, whereas in the absence of anionic lipids, the SecA-SecYEG interaction was completely absent (Fig. 1a) confirming our earlier report [14]. Some differences in binding affinity between the anionic lipids could be observed. In the presence of CL, the binding affinity of SecA to SecYEG nanodiscs was found to be slightly higher (K_D = 44.3 ± 24.3 nM) than with PA (K_D = 80.8 ± 31.4 nM) or PG (K_D = 102.7 ± 25.5 nM). A lower binding affinity was found in the presence of PS (K_D = 173.1 ± 44.7 nM). Overall the results show that SecA is stimulated for high affinity binding to SecYEG regardless of the anionic lipid species, and indicate SecA-membrane interaction is mainly charge dependent.

Next, the influence of the anionic lipid concentration in the membrane on the SecA-SecYEG interaction was examined. SecYEG was reconstituted in nanodiscs containing 0%, 5%, 10%, 20% or 30% PG, and the Kd of SecA binding to SecYEG was determined by MST (Fig. 1b). With increasing PG concentration from 0 to 10%, the measured Kd decreases, indicating that the amount of PG is limiting the SecA-SecYEG interaction. However, at PG concentrations above 10%, the Kd-value remain constant, hence an increase in the PG concentration does not further stimulate the SecA-SecYEG interaction. Another way to visualize this data is by plotting the fraction of SecYEG that has SecA bound in relation to the PG concentration (Fig. 1c, left Y-axis, open symbols). Above 10% PG the fraction bound is almost 1, implicating that virtually all translocons are occupied by SecA. Next, the influence of the anionic lipid concentration on the overall translocation process was determined. For this, a fluorescent proOmpA translocation assay was performed using SecYEG proteoliposomes. Here, proOmpA is translocated by SecYEG from the exterior into the lumen of the liposomes, and therefore is protected from degradation by the externally added Proteinase K. Translocation activity is determined by the percentage of translocated proOmpA. Remarkably, the translocation activity showed a different dependence on the PG concentration as compared to SecA-SecYEG binding, as translocation increased with the PG concentrations up to 30% (Fig. 1c, right Y-axis, filled symbols). This implies that even when SecA binding to SecYEG is fully saturated at 10% PG, the translocons are not yet fully functional, suggesting a second PG dependent step in the translocation mechanism.

This observation was confirmed by a SecA ATPase activity assay. The ATPase hydrolysis activity of SecA in the presence of proOmpA (translocation ATPase) was determined by measuring the free phosphate concentration using a malachite green reagent. Similar to the translocation activity, the ATP-hydrolysis showed a linear anionic lipid-dependency (Fig. 1d). This phenomenon was independent of the SecA concentration, *i.e.*, at non-saturating (50 nM) or saturating (500 nM) concentrations, thereby confirming that SecA-SecYEG binding and SecA mediated translocation are two distinct anionic lipid dependent processes.

2.2. Translocation activity can be restored by introducing newly synthesized anionic lipid

Although lipid-protein interactions in general are transient and dynamic, it cannot be excluded that anionic lipids play a permanent role in the structural organization of the translocon. For this reason, we want to exclude that the observed PG concentration-dependent effects are caused by structural and/or functional deficiencies during liposomal reconstitution of purified SecYEG. To examine this, anionic phospholipids were reintroduced in an anionic deficient membrane, for which we made use of a recently developed *in vitro* system for the enzymatic synthesis of PG [17]. In a cascade of enzymatic conversions, oleic acids and glycerol 3-phosphate are converted into the anionic phospholipid PG. As the oleic acid partitions into the existing lipid bilayer of the SecYEG proteoliposomes, conversion directly leads to the incorporation of PG into the existing proteoliposomal membrane (Fig. 2a). The presence of the translocon did not interfere with *in vitro* phospholipid biosynthesis and all oleic acid was converted into PG, with under the experimental conditions employed, to a maximum of 25% of total phospholipid (Fig. 2b). To determine whether the newly synthesized PG enables the restoration of SecYEG activity, an *in vitro* proOmpA translocation was performed (Fig. 2c). Introduction of PG into PE:PC proteoliposomes restored translocation up to 75% compared to synthetic PG:PE:PC (30:30:40 molar ratio) proteoliposomes, whereas proteoliposomes without PG did not support translocation. Although, the majority of the oleic acid (99%) was converted into PG, the remaining oleic acid could have an effect on translocation. To exclude that the negative charge of oleic acid caused restoration of SecYEG activity, SecYEG proteoliposomes containing twice the amount of remaining oleic acid were prepared. As expected, those low traces of oleic acid did not induce protein translocation. These data demonstrate that the activity of the translocon can be restored by replenishing the acidic phospholipid content of the proteoliposomes. We therefore can exclude that the observed stimulation of translocon activity with increasing PG concentration is an artifact of reconstitution in an anionic lipid poor environment, implying that there is another anionic lipid-dependent event that can stimulate the translocon its activity.

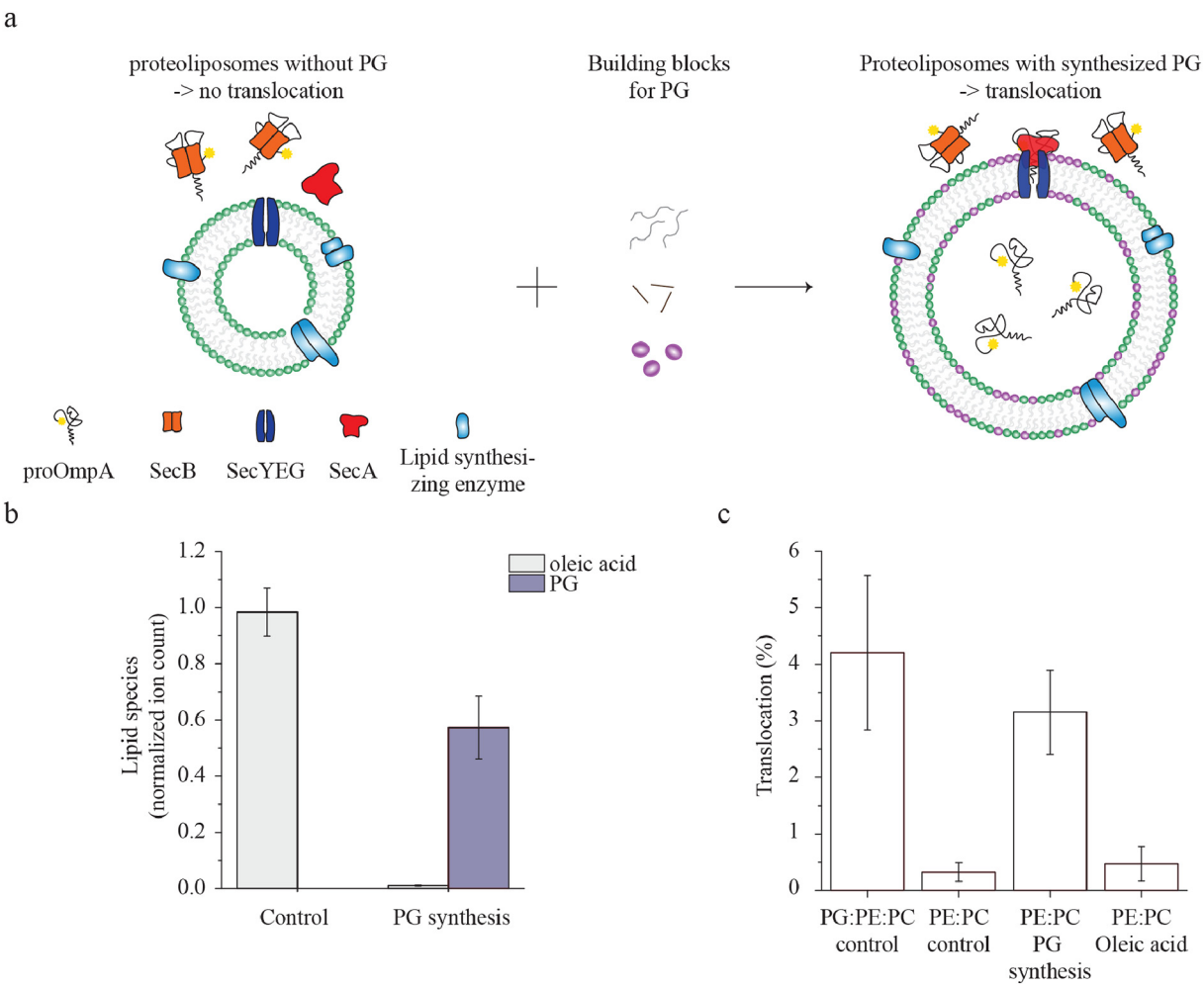

Fig. 2. SecYEG activity can be restored by anionic phospholipid generation. (a) Schematic representation of translocation restoration by introduction of the anionic lipid PG in PE:PC proteoliposomes reconstituted with SecYEG. Adapted from Exterkate and Driessen [18] (b) *In vitro* enzymatic synthesis of PG from oleic acid and glycerol 3-phosphate. Reactions were performed in the presence of purified enzymes reconstituted into SecYEG proteoliposomes. Products were analyzed by LC–MS, normalized for the internal standard and plotted. (**c**) *In vitro* proOmpA translocation assay with PE:PC proteoliposomes, in which PG was introduced (PE:PC:PG synthesis). Proteoliposomes with initial PG (PG:PE:PC control), without PG (PE:PC control) and with residual oleic acid (PE:PC:oleic acid) served as controls.

2.3. Exploring the second lipid-dependent step during translocation

To explore at the molecular level how anionic lipids influence translocation related events, other than the SecA-SecYEG interaction, coarse grain (CG) molecular dynamics simulations were performed in combination with the MARTINI force field. The use of a CG model provides access to longer time scales, which is required to interpret biological-related processes [19,20]. The MARTINI model, which maps on average four heavy atoms into an effective interaction site, has proven to be very efficient for this purpose [21–23].

First, the localization of anionic lipids in a membrane containing 10% PG was mapped, in which localization in the different leaflets was analyzed separately. In the cytoplasmic leaflet PG enriches around the embedded SecYEG-SecA complex, supporting our experimental data. In particular, two distinct high-density spots (green) can be identified around the SecYEG-SecA interface: close to the SecA N-terminus and near SecG (Fig. 3a, upper panel, site 1a and 1b respectively). In the periplasmic leaflet, two other PG-rich regions were observed: one near the loop between TMH5 and TMH6 of SecY (site 2), and one at the lateral gate (Site 3) (Fig. 3a, lower panel). Next, simulations were repeated in the presence of 30% PG. The anionic lipid density maps of both the periplasmic and cytoplasmic leaflet show an overall increase of PG, but no specific new PG-rich regions could be identified (Fig. 3a, right panels). Instead, PG seems to particularly accumulate at the earlier identified high-density spots. The PG molecules present in site 1a, 1b and 3, show a long (μs) life-time (Fig. 3b, depicted in red), thereby representing PG-binding sites. In fact, we observe that once associated, the binding of PG near the lateral gate is persistent till the end of the simulation (50 μs). On the other hand, PG residing at other locations around the translocon (including site 2) shows a much shorter life-time (ns life-time, depicted in green), displaying a more transient behavior. Other lipid species, *i.e.* PE, do not accumulate near the translocon (Fig. S1).

To validate our results obtained with the CG force field, MD simulations were continued from well-equilibrated configurations obtained at CG level, which were then back-mapped to AA representation. In line with the CG resolution, the AA simulations show that the PG binding spots are indeed preserved (Fig. S2). A detailed analysis of the SecA-SecYEG interface shows PG localizing in two distinct sites (1a and 1b), both in close proximity of SecG (Fig. S3). At site 1a, a PG molecule is sandwiched between the SecY and SecG interface and further stabilized by residues K54 (SecG) and R177 (SecY) (Fig. S3a). At site 1b, the lipid is interacting with the external face of SecG and additionally stabilized by the N-terminal residue M1 of SecA (Fig. S3b), thereby representing the binding site for the SecA N-terminus. Interestingly, an important role of the N-terminus of SecA in the interaction with SecG has been reported earlier [24]. From these observations, we conclude that the interactions at site 1a and 1b are specific for anionic phospholipids. A

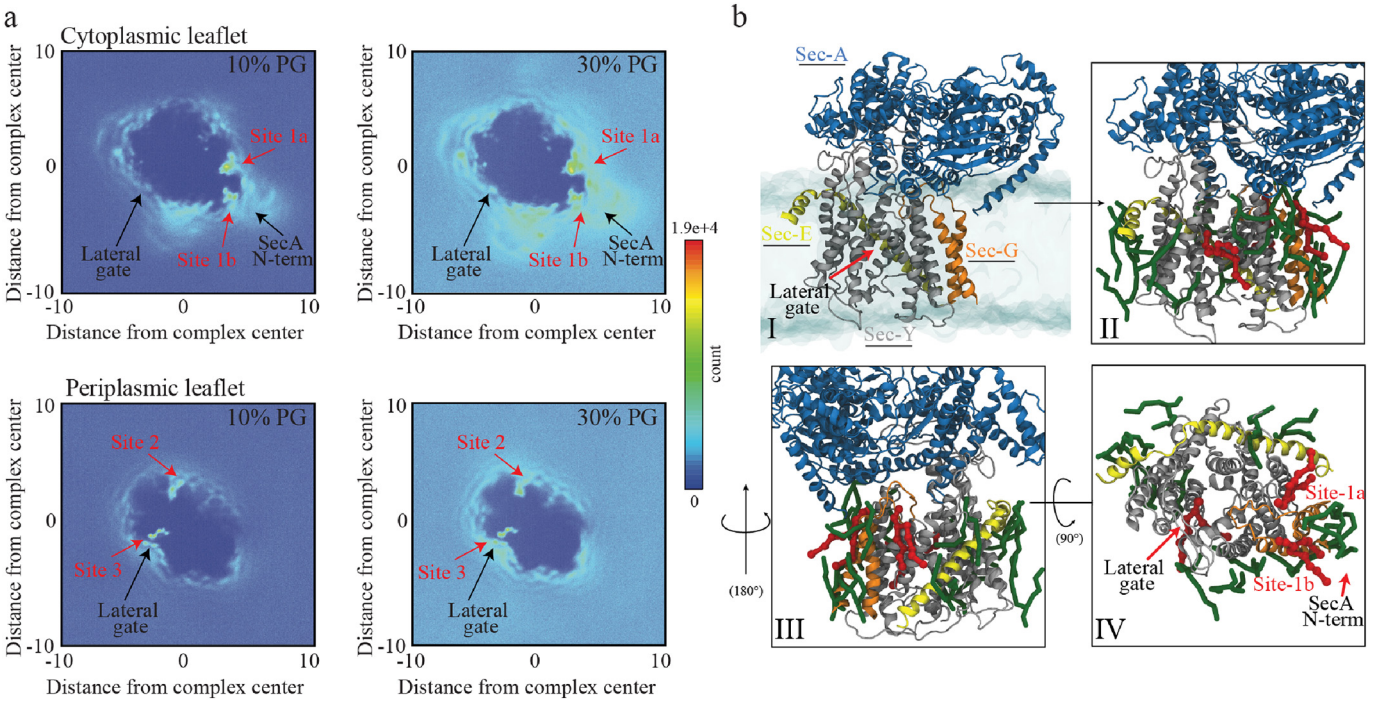

Fig. 3. Simulation of anionic lipid-enrichment around the SecYEG channel. (a) 2D density map of anionic lipids (PG) around the SecY-SecA complex viewed from the cytoplasmic and periplasmic side of the membrane, in the presence of 10% and 30% PG (left and right panel, respectively). (b) Long-live localization of anionic lipids around the SecY-SecA complex. (I) Topology of the SecY-SecA complex. The structure highlights SecY (grey ribbons), SecG (orange ribbons), SecE (yellow ribbons) and SecA (blue ribbons). (II) Lateral view of the complex with accompanied PG lipids. Two sets of anionic lipids can be identified: green lipids (ns life-time) and red lipids (μs life-time). Lipids were identified using the density map provided in (A) (III) Idem as II but rotated 180° around the Z axis. (IV) 90° rotation around the X axis with respect to (III). Three long life-time binding sites for PG (red) have been identified: one within the lateral gate and two near SecG and the SecA N-terminus (namely site-1 and site-2).

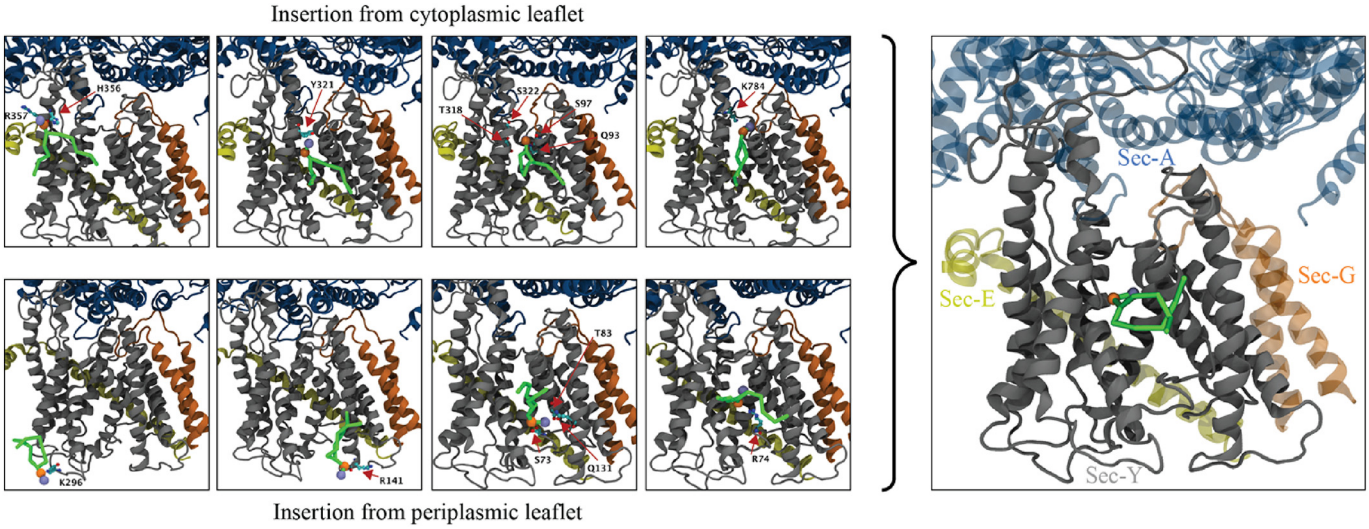

Fig. 4. Anionic lipid positioning at the lateral gate. Insertion of PG (green) into the lateral gate of SecY (grey) originating from the cytoplasmic (upper panel) or the periplasmic leaflet (lower panel). SecA, SecE and SecG are shown in blue, yellow and orange, respectively. Specific interactions with polar and positively charged amino acid side chains of SecY are highlighted. PG reaches its final position between the acyl chains of the anionic lipid and TMH2b (red oval), TMH7 (blue oval) and TMH8 (green oval) (right panel), regardless from which membrane leaflet the lipid molecule originates.

high stabilization of PG in these sites is given by salt-bridges between specific basic residues and the charged phospholipid headgroup, as well as hydrophobic amino acids that are in contact with the PG acyl-chains.

PG is further enriched in the periplasmic leaflet of the membrane close to the loop between TMH5 and TMH6 of SecY (site 2) and near the lateral gate between TMH 7, TMH8 and 2b of SecY (site 3). Although the functioning of the loop connecting TMH5 and TMH6 of SecY in translocation is unknown, the lateral gate was identified earlier to participate in this process. During translocation of preproteins, the structural conformation of the lateral gate changes from a closed *via* a pre-open to an open state [4,8,25], which should allow for interactions of surrounding lipids with the interior of the translocating channel. Our simulations show for the first time that PG is located at the lateral gate and partially inserts into the channel in the middle of the lateral gate (Fig. 4, big panel). Here, the phospholipid is stabilized by persistent binding regions within the lateral gate (one within TMH 7, one within

TMH 8 and one within TMH 2b of SecY) (Fig. S4). Noteworthy, the simulations show that lipids enter the lateral gate from both the periplasmic leaflet (Fig. 4, upper panels and Movie S1) as well as the cytoplasmic leaflet, *via* two distinct routes. As lipids from both leaflets end up in the same position with the same orientation, this implies that PG originating from the periplasmic leaflet performs a complete flip-flop (Fig. 4, lower panels and Movie S2). Remarkably, repeated simulations (10 replicas) show that in the presence of 10% PG there is no preference for PG entering the lateral gate originating from the periplasmic or the cytoplasmic leaflet. On the other hand, in the presence of 30% PG, in only 2 out of 10 replicas the PG enters from periplasmic leaflet, indicating specificity for the cytoplasmic leaflet. Summarizing, an increase of the PG concentration to 30% did not result in additional PG crowding spots, but rather increased the anionic lipid enrichment also identified at 10% PG concentration. This is in accordance with the experimental data, which show a gradual increase in translocation with the PG concentration, instead of a critical threshold concentration that activates the translocation process.

We further studied the preferential anionic lipid association of the SecA-SecYEG complex by performing simulations with membranes containing both PG and CL lipids (see Methods). The average number of lipids around the translocon within 1 nm lateral range was computed and plotted (Fig. S5). At a first glance there seems to be no specific preference for either PG or CL, as the translocon is surrounded by an equimolar amount of anionic lipids. However, by mapping the individual lipid density of PG and CL respectively, it becomes clear that these lipids species associate with the translocon at distinct sites (Fig. 5a). PG is more enriched around the SecY domain, whereas CL preferentially associates with the SecA domain (cytoplasmic leaflet). This observation becomes even more evident by examining the periplasmic leaflet, where hardly any CL is localized near the SecY domain, suggesting that the interaction with the complex is not solely a charge-charge compensation, but has lipid specificity. In the absence of PG, CL localizes at the earlier identified regions around the SecA N-terminus (site 1a/b) and in addition to the lateral gate (site 3), but not around site 2, suggesting again a lipid specific recognition, which can't be totally compensated by charge.

Focussing on the SecA-SecYEG binding site, CL shows similar interactions compared to PG, except for the nucleotide binding site 2 (NBD2) subdomain of SecA. As indicated by our simulations, PG lipids interact shortly with this region while CL lasts longer, clearly suggesting a long-live association region (Fig. S6). Binding of PG and CL in the proximity of the lateral gate shows a more pronounced difference. Although CL localizes in the proximity of the lateral gate, it is unable to deeply interact with the channel itself. There seems to be a limited mass-size that the lateral gate can accept and divalent lipids like CL are too bulky to get in there.

3. Discussion

Anionic phospholipids are essential components of the phospholipid membrane and amongst others, are crucial for protein translocation. One of these anionic lipid dependent events in translocation is the binding of SecA to SecYEG. Here we further elaborated on the role of anionic lipids in this process and studied the impact on the overall translocon activity. The SecA N-terminus plays an important role in SecA-SecYEG binding, as it is vital for the initial association of SecA with the membrane, and precedes the high-affinity binding of SecA to

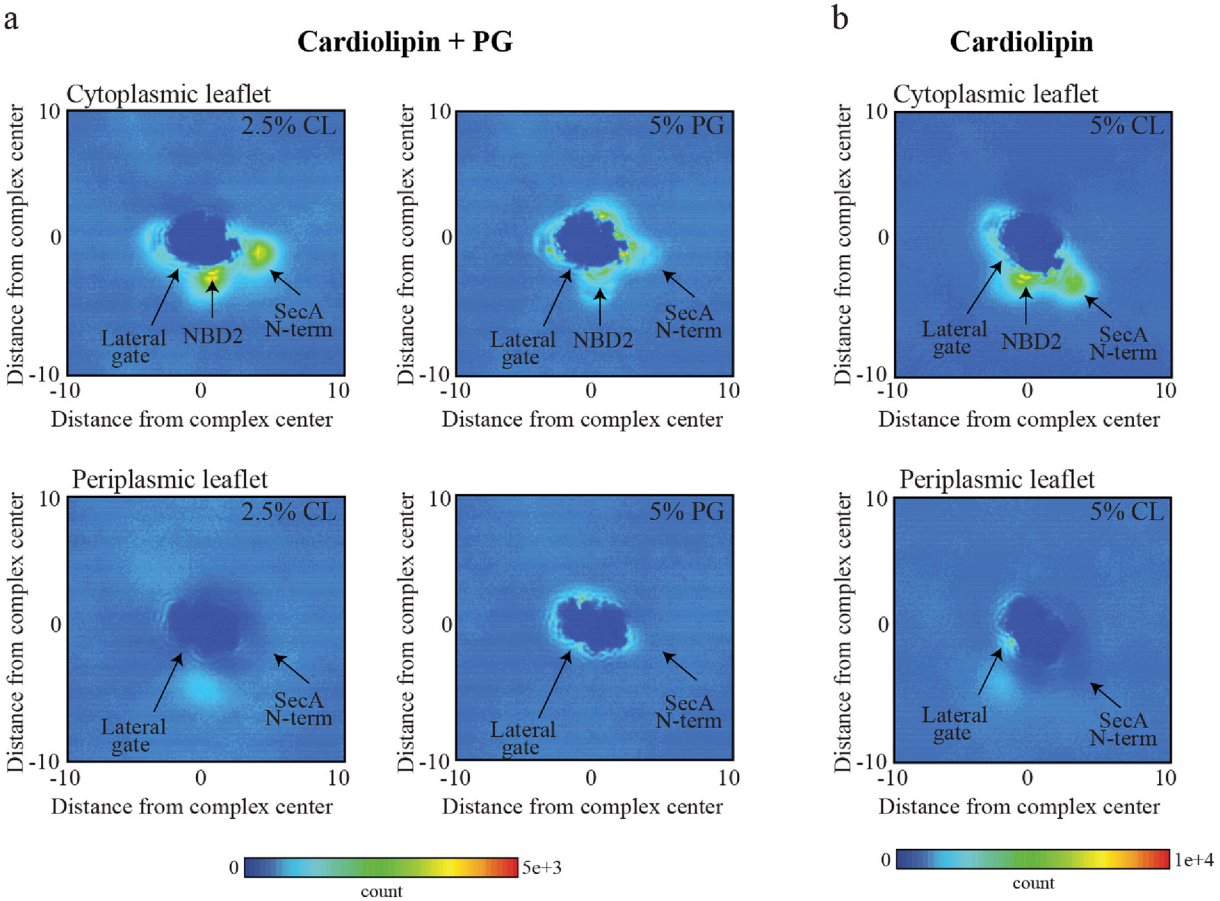

Fig. 5. Simulation of anionic lipid-enrichment around the SecYEG channel. a) 2D density map of CL in a membrane containing only this anionic lipid. b) 2D density map of CL (left panels) and PG (right panels) in a membrane containing both anionic lipids. Localization around the SecY-SecA complex is displayed for the cytoplasmic (upper panels) and periplasmic side (lower panels) of the membrane.

SecYEG. This binding reaction is believed to be mainly electrostatic, implying that it is not dependent on a specific lipid type, but can be established in the presence of any anionic lipid species. Indeed, we observe that SecYEG complexes associate with SecA, regardless of the anionic lipid species present in the nanodiscs. With PS, a lower binding affinity was observed. PS is overall negatively charged, but contains a polar head group. This could form a charge- and spatial-dependent obstruction for the insertion of the positively charged N-terminus of SecA parallel into the membrane [26], and could explain the lower affinity of SecA for SecYEG in PS containing membranes. It should be noted that PS is an intermediate in PE formation and it is only present in *E. coli* membranes in minute amount. Thus, the lower affinity of SecA binding with PS likely has little physiological relevance. With cardiolipin (CL), the binding affinity is almost twice as good as with PG or PA. CL contains two negative charges, resulting in a smaller anionic surface area compared to PA or PG. This could explain why SecA binding to SecYEG nanodiscs containing CL is enhanced relative to either PG or PA. This observation is supported by our MD simulations, that clearly show that CL is directly involved in stabilizing the association of SecA with the membrane. This could potentially increase the local concentration of SecA within the boundaries of a pre-embedded SecYEG complex. Although PG is also able to provide a similar stabilizing mechanism, CL enhances such process through a tighter binding to both the N-terminal as well as the NBD2 region of SecA.

Although the anionic lipid type mildly influences the SecA-SecYEG association, the concentration of anionic lipid has a clear effect on this interaction. The binding increases with the PG concentration up to 10%, after which binding saturates. On the other hand, translocation activity did not reach a plateau at 10% PG, but increased further with higher PG concentrations. This is further supported by the observation that newly synthesized PG [17] introduced into an anionic lipid deficient membrane restored the translocation activity to the levels expected for the realized anionic lipid concentration (25%). Restoration of translocation implies a dynamic lipid-translocon interplay and excludes any permanent structural deficiencies of the translocon during the reconstitution in an anionic lipid deficient membrane. Since the enhanced translocation activity at concentrations of anionic lipids above 10% cannot be attributed to improved SecA-SecYEG binding, there must be another translocation related event that is dependent on the anionic lipid concentration.

By using translocons embedded in lipid bilayer particles encircled by SMA (styrene maleic acid) polymers, we have previously shown that anionic phospholipids form an annulus around the SecYEG channel [10]. Thus, the second anionic lipid dependent reaction may relate to the translocon-lipid reaction. Therefore, computational analysis was performed on a membrane embedded SecYEG-SecA complex. Here, we were able to identify specific interaction sites of PG with SecYEG. We observed accumulation of anionic lipids in the cytoplasmic leaflet at two distinct spots close to the SecYEG-SecA complex. As expected, one spot is located near the SecG and SecA-N-terminus interface, representing anionic lipid mediated SecA association with SecYEG (site 1b). Interestingly, the second binding site was found close to the first binding site at the interface between SecG and SecY, again indicating a dominant role for SecG in the SecA-SecYEG interaction (site 1a). Previously, it was shown that SecG is not essential for protein translocation, but its deletion results in a cold-sensitive growth defect that can be attributed to impaired secretion [27]. Remarkably, this phenomenon could be suppressed by the overexpression of the *pgsA* gene that encodes for an enzyme responsible for PG synthesis [28]. Thus, elevated PG concentrations can suppress the SecG deficiency. Moreover, SecG is believed to contribute to the binding of SecA to the translocon [29]. Hence, the presence of acidic phospholipids in the vicinity of SecG suggests a potential role in facilitating the anionic lipid-dependent binding of SecA to the translocon. Both of these anionic lipid binding sites highlighted in this study, have also been identified to bind CL in a recent study [30]. By mutating the positive charges within TMH 1 and 4, corresponding to the binding sites at the interface between SecG and SecY, a reduction of the binding affinity for CL was detected. Although these binding sites were suggested to be specific for interactions with CL, our study demonstrates that both CL and PG interact with the same sites. The fact that there seems to be a preference for CL, when both lipid species are present does not mean there is a specific dependence on CL. This study, as well as previous *in vitro* and *in vivo* studies, show that in translocation the negative charge of anionic lipids is mainly decisive for SecA targeting and protein translocation and not so much the type of anionic lipid [10,31].

Two additional anionic lipid binding hotspots were identified at the periplasmic leaflet of the translocon. One of these spots concerns a close interaction of anionic lipids with the loop between TMH5 and TMH6 of SecY (site 2), which according to our MD data, seems to be exclusive for PG. As there is no known function of these interactions, the purpose of anionic lipid binding in this region remains unclear. However, the other hot-spot is located near the lateral gate (site 3), which is known to switch from a closed to an open state at the initiation of protein translocation. Although both PG and CL are able to accumulate within this region, there seems to be a preference for PG when both of these anionic species are present. PG inserts with its polar headgroup into the opened lateral gate, a phenomenon that is not observed with CL. As the gate extends across the lipid bilayer, it allows for entry from both leaflets, which would involve flip-flop for lipids entering from the periplasmic leaflet. Remarkably, a preference for lipids originating from the cytoplasmic leaflet can be observed, depending on the PG concentration. Although these findings are merely predictive and PG specific, they do provide an indication that the other anionic lipid-dependent event in post-translational translocation may involve interactions with the lateral gate. This is supported by other data showing that TMH 2 and 3 of the lateral gate are involved in anionic lipid binding [30], and that opening of the lateral gate is critical for protein translocation [7]. In this respect, a mutational study of the eukaryotic Sec61 which is homologous to SecY showed substrate targeting and membrane insertion defects when T87 and Q93 were substituted by alanine residues [32], two amino acid residues that in our study were identified for PG-positioning within the lateral gate (Fig. 4).

Finally, our simulations show that the interactions of phospholipid with the lateral gate are exclusively achieved by anionic lipids, in which the negatively charged headgroup inserts into the lateral gate, allowing for electrostatic interactions with complementary molecules. The most likely candidate for such interactions is the signal sequence of preproteins. It has been proposed that the lateral gate plays a role for signal sequence binding of preproteins [8]. Signal sequences usually consist of a positively charged N-terminus, a hydrophobic core of 7–15 amino acids and a polar C-terminus of 3–7 residues [33]. Anionic lipids have been shown to promote α-helix formation of signal peptides and cause the signal sequence to bind to the membrane [34,35]. Interestingly, induction of complete α-helical conformation was only observed at a critical anionic lipid concentration of 35% and in the absence of salt. When positive charges at the N-terminus of the signal peptide are replaced with negative charges, the interaction of the signal peptide with the lipids was impaired [36], and this disrupts the function of these signal peptides to support translocation. Our results suggest that the signal sequence - anion lipid interaction is orchestrated at the lateral gate of SecY and that anionic lipid crowding in the gate can stimulate signal peptide positioning.

4. Materials and methods

4.1. Protein production and purification

All strains and plasmids used in this study are listed in Table 1. SecA was overexpressed in *E. coli* BL21 (DE3) and purified from the cytoplasm as described [14,37]. The extinction coefficient used for SecA at 280 nm was 75,750 M^{-1} cm^{-1}.

Table 1
List of strains and plasmids used in this study.

Strain/plasmid	Short description	Source
E. coli strain		
DH5α	F-, *endA1*, *glnV44*, *thi-1*, *recA1*, *relA1*, *gyrA96*, *deoR*, *nupG*, *Φ80dlacZΔM15*, Δ(*lacZYA-argF*)*U169*, *hsdR17*(*rK-mK+*), λ−	[38]
SF100	F-, *lacX74*, *galE*, *galK*, *thi*, *rpsL* (*strA*), Δ*phoA*(*pvuII*), Δ*ompT*	[39]
BL21(DE3)	F- *ompT* *hsd*SB(rB–, mB–) *gal dcm* (DE3)	[40]
Plasmids		
pEK20-C148	SecY (L148C)EG	[41]
pET502	proOmpA (C302S, C290)	[42]
pTrc99 SecA	SecA	[14]

E. coli DH5α harboring pET502 encoding for single-cysteine mutated proOmpA was grown at 37 °C until an OD_{600} of 0.6, whereupon protein expression was induced by addition of 0.5 mM IPTG. After 2 h of growth, cells were harvested at 6000 ×*g* for 15 min at 4 °C, washed in 50 mM Tris/HCl, pH 7, spun down at 12,000 ×*g* and resuspended in 50 mM Tris/HCl, pH 7. After cell lysis, inclusion bodies were collected at 2000 ×*g* for 10 min and solubilised in the presence of 8 M urea. Anion exchange was performed for proOmpA purification as explained previously [43]. Single cysteine mutated proOmpA was labelled with fluorescein and free dye was removed by TCA precipitation.

SecYEG was overexpressed in *E. coli* SF100 and purified from crude membranes using Ni+ affinity chromatography as described previously [13]. For fluorescent labelling, 1 mg Ni^{+}-NTA bound SecYEG was incubated with Cy5 according to manufacturer's manual (GE Healthcare) for 2 h at 4 °C. Free dye was removed using washing buffer containing 50 mM Tris/HCl pH 7, 100 mM KCl, 0.1% DDM, 10 mM Imidazole and 20% (v/v) Glycerol. SecYEG was eluted using 300 mM imidazole. The purity and concentration of SecYEG and the fluorophore was estimated by SDS-PAGE and spectrophotometrically. The extinction coefficient used for SecYEG at 280 nm was 71,000 M^{-1} cm^{-1}. The extinction coefficients for the fluorophores were used as provided by the manufacturers.

The scaffold protein ApoE422k consisting of the 22 kDa N-terminal fragment of the human apolipoprotein E4 linked to a 6-His and thioredoxin (Trx) tag was overexpressed and purified as described [44].

4.2. Reconstitution of SecYEG into proteoliposomes

To form liposomes containing varying anionic lipid concentrations, 0% PG (DOPC:DOPG:DOPE molar ratio 70:0:30), 5% PG (DOPC:DOPG:DOPE molar ratio 65:5:30), 10% PG (DOPC:DOPG:DOPE molar ratio 60:10:30), 20% PG (DOPC:DOPG:DOPE molar ratio 50:20:30) and 30% PG (DOPC:DOPG:DOPE molar ratio 40:30:30) lipid mixtures were prepared (Avanti Biochemicals, Birmingham, USA). To prepare liposomes containing varying types of anionic lipids, DOPC and DOPE were either mixed with DOPG, DOPA or DOPS in a molar ratio 40:30:30. Due to the presence of 2 negative charges, DOPC:CL:DOPE lipid mixtures were prepared with a molar ratio 40:15:30. Lipid mixtures were dried under a nitrogen stream and remaining traces of chloroform were removed by further drying of the lipid film in a desiccator overnight. Lipids were resuspended in a buffer containing 20 mM Tris/HCl, pH 8, 2 mM DTT and sonicated. Lipids were solubilised in 0.5% Trition X-100 and mixed with 2.5 nmol purified SecYEG. Reconstitution was performed as described before [45].

4.3. Reconstitution of SecYEG into nanodiscs

For nanodiscs preparation, lipid mixtures were prepared and solubilised as explained for SecYEG proteoliposomes. SecYEG was mixed with a buffer containing 50 mM Tris/HCl, pH 8, 50 mM KCl, 0.1% DDM, 20% glycerol to a final volume of 1 mL. To achieve a monomeric state of the translocase, SecYEG, ApoE422k and lipids in a molar ratio of 0.25:10:1800 and incubated 4 °C for 1 h. Detergent was removed in 3 steps of 1.5 h with 50 mg, 75 mg and 100 mg Bio-Beads SM2 sorbent (Bio-Rad), whereby the last incubation was performed overnight. Formed proteoliposomes were removed by a centrifugation at 250,000 x*g* for 30 min. The nanodiscs were concentrated using Amicon® Ultra-4 50 K Centrifugal Filter Devices and subjected to size-exclusion chromatography by fast protein liquid chromatography using a Superose 6 column (GE Healthcare). 0.5 mL elution fractions were collected in 50 mM HEPES/KOH, pH 7.4, 100 mM KCl, and 5% glycerol. Nanodisc containing fractions were analyzed by SDS-PAGE.

4.4. In vitro proOmpA translocation assay

The translocation activity of SecYEG in the presence of varying anionic lipid types and concentrations, was determined by a proOmpA translocation and protease protection assay as described [46]. ProOmpA was fluorescently labelled using fluorescein and translocated fluorescent proOmpA was detected in glycine gel using a Biomolecular-imager (LAS 4000 Fujifilm).

4.5. ATPase assay

The ATPase activity of SecA in the presence of SecYEG proteoliposomes consisting of different anionic lipid types and concentrations, was analyzed as described [14].

4.6. Microscale thermophoresis

To investigate the binding of SecA to SecYEG nanodiscs harboring varying anionic lipid types and concentrations, Microscale Thermophoresis was performed using a Monolith NT.115 from Nanotemper Technologies (Munich, Germany) as described [14]. Data were fitted using the law of mass action.

4.7. In vitro assays for phospholipid production

The *in vitro* biosynthesis of phospholipids was done as described before, employing purified phospholipid biosynthesis enzymes as detailed elsewhere [22]. In short, all reactions were performed in 100 µL of Assay Buffer containing a final concentration of 50 mM Tris/HCl, pH 8.0, 10 mM $MgCl_2$, 100 mM KCl, 15% glycerol and 2 mM DTT. Conversion of oleic acid into PG was assayed in buffer A with addition of 0.5 µM FadD, 50 µM CoA, 2250 µM oleic acid, 4 mM ATP, 3.5 mM SecYEG proteoliposomes, 10 mM G3P, 0.5 µM PlsB, 1.5 µM PlsC, 2 µM CdsA, 3 mM CTP, 1 µM PgsA and 1 µM PgpA. All reactions were incubated overnight at 37 °C. Lipids were extracted two times with 0.3 mL of n-butanol, and evaporated under a stream of nitrogen gas and resuspended in 50 µL of methanol for LC–MS analysis.

4.8. LC-MS analysis of lipids

Samples from the *in vitro* reactions were analyzed using an Accela1250 HPLC system coupled with an ESI–MS Orbitrap Exactive (Thermo Fisher Scientific) as described [47]. In short, 5 µL was injected into a COSMOSIL 5C4-AR-300 Packed Column, 4.6 mm I.D. × 150 mm (Nacalai USA, Inc.) operating at 40 °C with a flow rate of 500 µL/min. Separation of the compounds was achieved by a changing gradient of Mobile phase A (50 mM ammonium bicarbonate in water) and mobile phase B (Acetontrile). The MS settings and specifications used for this analysis were the same as described before [47].

Spectral data constituting total ion counts were analyzed using the Thermo Scientific XCalibur processing software by applying the Genesis algorithm based automated peak area detection and integration. The total ion counts of the extracted lipid products: oleic acid (*m/z* 281.25 $[M - H]^{-}$), DOPG (*m/z* 773.53 $[M - H]^{-}$), were normalized for the

internal standard DDM (m/z 509.3 $[M - H]^-$) and plotted on the y-axis as normalized ion count.

4.9. Molecular dynamics

The GROMACS MD engine (version 5.1.2) [48] was used in combination with the MARTINI 2.2 force field for running all coarse-grain (CG) simulations [49]. The atomic coordinates of the SecYEG-SecA complex (**PDB ID 3DIN**) were downloaded and transformed into CG representation using the *martinize* script [50]. An internal elastic network was applied along the backbone beads of the complex in order to improve general stability [51]. The complex was embedded in pre-equilibrated membrane patches containing DOPC-DOPE-DOPG either at 40-30-30 (504-378-378 lipids respectively) or 60-30-10 (756-378-126 lipids respectively) lipid ratios. In addition, extra runs were also performed with membranes in which PG was partially (3 replicates) or completely (3 replicates) replaced by cardiolipin (CL). In agreement with simulations using one anionic lipid species, the overall anionic content was kept constant at 10% using membranes containing either 5% CL, or a combination of 5% PG + 2,5% CL. The systems were run at neutral charge balance by adding Na + ions. We followed a current update in parameters set-up for performing the simulations [52]. Equations of motion were integrated using a 30 fs time-step. Reaction-field electrostatics was used with a Coulomb cut-off of 1.1 nm and dielectric constants of 15 or ∞ within or beyond this cut-off, respectively. A cut-off of 1.1 nm was also used for calculating Lennard-Jones interactions, using a scheme that shifts the Van der Waals potential to zero at this cut-off. Constant temperature was maintained at 310 K *via* separate coupling of the solvent and membrane/protein components to velocity rescaling thermostat with a relaxation time of 1.0 ps. During equilibration, the system pressure was coupled using a semi-isotropic pressure approach at 1 bar using a Berendsen barostat with a relaxation time of 12.0 ps. Position restraints were applied only to protein beads (backbone and side chain) during the entire equilibration using a force constant of 1000 kJ/mol·nm^2. During production time, a Parrinello pressure barostat was applied with relaxation time of 12.0 ps and no restraints were used on the dynamics of the protein. Equilibration time (2 μs) was followed by production time (50 μs) and trajectories were saved every 3 ns for analysis using pre-compiled GROMACS tools.

In order to validate the CG predictions, an equilibrated frame from the CG simulations (all anionic binding sites occupied) was back-mapped [53] into all atom (AA) resolution using the charmm36m force field [54]. The fully atomic representation contained ~0.7 M particles which were energy minimized before production runs. The water model is represented by the TIP3P [55] with CHARMM modifications [56]. Water molecules are rigidified with SETTLE [57], and bonds involving hydrogen in lipids and proteins are constrained with P-LINCS [58]. Lennard-Jones interactions are evaluated using an atom-based cutoff, gradually switching off forces between 1.0 and 1.2 nm. Coulomb interactions beyond 1.2 nm are calculated using the smooth particle-mesh Ewald (PME) method [59]. Membranes were semi-isotropically coupled to a *NpT* ensemble *via* a Parrinello-Rahman barostat [60] at 1 atm. The temperature of the system was maintained to 310 K using the V-rescale approach [61], with a coupling constant of 1 ps. Simulations were run for 0.3 μs and trajectories were saved every 200 ps for analysis.

Supplementary data to this article can be found online at https://doi.org/10.1016/j.bbamem.2019.183035.

Accession numbers

PDB ID: 3DIN

Transparency document

The Transparency document associated with this article can be found, in online version.

Declaration of competing interest

The authors declare no conflicts of interest.

Acknowledgements

Funding

The work was financially supported by the Foundation for Fundamental Research on Matter (FOM).

Author contributions using CRediT

Sabrina Koch and Marten Exterkate: Conceptualization, Methodology, Validation, Formal Analysis, Investigation, Visualization, Writing – original draft. **Cesar A. López:** Conceptualization, Methodology, Software, Validation, Formal Analysis, Investigation, Visualization, Writing – original draft. **Megha Patro:** Validation, Formal Analysis, Investigation, Visualization. **Siewert J. Marrink:** Writing – Reviewing and Editing. **Arnold J.M. Driessen:** Conceptualization, Writing – Reviewing and Editing, Supervision, Funding Acquisition.

References

[1] A.J.M. Driessen, N. Nouwen, Protein translocation across the bacterial cytoplasmic membrane, Annu. Rev. Biochem. 77 (2008) 643–667, https://doi.org/10.1146/annurev.biochem.77.061606.160747.
[2] F.U. Hartl, S. Lecker, E. Schiebel, J.P. Hendrick, W. Wickner, The binding cascade of SecB to SecA to SecY/E mediates preprotein targeting to the E. coli plasma membrane., Cell. 63 (1990) 269–79. doi:https://doi.org/10.1016/0092-8674(90)90160-G.
[3] L. Brundage, J.P. Hendrick, E. Schiebel, A.J.M. Driessen, W. Wickner, The purified E. coli integral membrane protein SecY/E is sufficient for reconstitution of SecA-dependent precursor protein translocation., Cell. 62 (1990) 649–57. doi:https://doi.org/10.1016/0092-8674(90)90111-Q.
[4] B. van den Berg, W.M. Clemons, I. Collinson, Y. Modis, E. Hartmann, S.C. Harrison, T.A. Rapoport, X-ray structure of a protein-conducting channel, Nature. 427 (2004) 36–44, https://doi.org/10.1038/nature02218.
[5] E. Schiebel, A.J.M. Driessen, F.U. Hartl, W. Wickner, ΔμH+ and ATP function at different steps of the catalytic cycle of preprotein translocase, Cell. 64 (1991) 927–939, https://doi.org/10.1016/0092-8674(91)90317-R.
[6] J.P.W. van der Wolk, J.G. de Wit, A.J.M. Driessen, The catalytic cycle of the Escherichia coli SecA ATPase comprises two distinct preprotein translocation events, EMBO J. 16 (1997) 7297–7304, https://doi.org/10.1093/emboj/16.24.7297.
[7] D.J.F. du Plessis, G. Berrelkamp, N. Nouwen, A.J.M. Driessen, The lateral gate of SecYEG opens during protein translocation, J. Biol. Chem. 284 (2009) 15805–15814, https://doi.org/10.1074/jbc.M901855200.
[8] L. Li, E. Park, J.J. Ling, J. Ingram, H. Ploegh, T.A. Rapoport, Crystal structure of a substrate-engaged SecY protein-translocation channel, Nature. 531 (2016) 395–399, https://doi.org/10.1038/nature17163.
[9] P.C.K. Tam, A.P. Maillard, K.K.Y. Chan, F. Duong, Investigating the SecY plug movement at the SecYEG translocation channel, EMBO J. 24 (2005) 3380–3388, https://doi.org/10.1038/sj.emboj.7600804.
[10] I. Prabudiansyah, I. Kusters, A. Caforio, A.J.M. Driessen, Characterization of the annular lipid shell of the Sec translocon, Biochimica et Biophysica Acta (BBA) - Biomembranes. 1848 (2015) 2050–2056. doi:https://doi.org/10.1016/j.bbamem.2015.06.024.
[11] T. de Vrije, R.L. de Swart, W. Dowhan, J. Tommassen, B. de Kruijff, Phosphatidylglycerol is involved in protein translocation across Escherichia coli inner membranes, Nature. 334 (1988) 173–175, https://doi.org/10.1038/334173a0.
[12] R. Lill, W. Dowhan, W. Wickner, The ATPase activity of SecA is regulated by acidic phospholipids, SecY, and the leader and mature domains of precursor proteins., Cell. 60 (1990) 271–280. doi:https://doi.org/10.1016/0092-8674(90)90742-W.
[13] C. van der Does, J. Swaving, W. van Klompenburg, A.J.M. Driessen, Non-bilayer lipids stimulate the activity of the reconstituted bacterial protein translocase, J. Biol. Chem. 275 (2000) 2472–2478, https://doi.org/10.1074/jbc.275.4.2472.
[14] S. Koch, J.G. de Wit, I. Vos, J.P. Birkner, P. Gordiichuk, A. Herrmann, A.M. van Oijen, A.J.M. Driessen, Lipids activate SecA for high affinity binding to the SecYEG complex, J. Biol. Chem. 291 (2016) 22534–22543, https://doi.org/10.1074/jbc.M116.743831.
[15] B. Bauer, T. Shemesh, Y. Chen, T.A. Rapoport, A push and slide mechanism allows sequence-insensitive translocation, Cell. 157 (2014) 1416–1429, https://doi.org/10.1016/j.biotechadv.2011.08.021.Secreted.
[16] E. Breukink, R.A. Demel, G. de Korte-Kool, B. de Kruijff, SecA insertion into phospholipids is stimulated by negatively charged lipids and inhibited by ATP: a

monolayer study, Biochemistry. 31 (1992) 1119–1124, https://doi.org/10.1021/bi00119a021.
[17] M. Exterkate, A. Caforio, M.C.A. Stuart, A.J.M. Driessen, Growing membranes in vitro by continuous phospholipid biosynthesis from free fatty acids., ACS Synthetic Biology. 7 (2018) 153–165. doi:https://doi.org/10.1021/acssynbio.7b00265.
[18] M. Exterkate, A.J.M. Driessen, Synthetic minimal cell: self-reproduction of the boundary layer, ACS Omega. 4 (2019). doi:https://doi.org/10.1021/acsomega.8b02955.
[19] G. Hedger, M.S.P. Sansom, Lipid interaction sites on channels, transporters and receptors: recent insights from molecular dynamics simulations, Biochim. Biophys. Acta Biomembr. 1858 (2016) 2390–2400, https://doi.org/10.1016/j.bbamem.2016.02.037.
[20] H.I. Ingolfsson, C. Arnarez, X. Periole, S.J. Marrink, Computational microscopy of cellular membranes, J. Cell Sci. 129 (2016) 257–268, https://doi.org/10.1242/jcs.176040.
[21] F.J. van Eerden, M.N. Melo, P.W.J.M. Frederix, S.J. Marrink, Prediction of thylakoid lipid binding sites on photosystem II, Biophys. J. 113 (2017) 2669–2681, https://doi.org/10.1016/j.bpj.2017.09.039.
[22] R.X. Gu, H.I. Ingólfsson, A.H. De Vries, S.J. Marrink, D.P. Tieleman, Ganglioside-lipid and ganglioside-protein interactions revealed by coarse-grained and atomistic molecular dynamics simulations, J. Phys. Chem. B 121 (2017) 3262–3275, https://doi.org/10.1021/acs.jpcb.6b07142.
[23] C. Arnarez, S.J. Marrink, X. Periole, Molecular mechanism of cardiolipin-mediated assembly of respiratory chain supercomplexes, Chem. Sci. 7 (2016) 4435–4443, https://doi.org/10.1039/C5SC04664E.
[24] H. Mori, H. Sugiyama, M. Yamanaka, K. Sato, M. Tagaya, S. Mizushima, Amino-terminal region of SecA is involved in the function of SecG for protein translocation into Escherichia coli membrane vesicles, J. Biochem. 124 (1998) 122–129, https://doi.org/10.1093/oxfordjournals.jbchem.a022070.
[25] J. Zimmer, Y. Nam, T.A. Rapoport, Structure of a complex of the ATPase SecA and the protein-translocation channel, Nature. 455 (2008) 936–943, https://doi.org/10.1038/nature07335.
[26] B.T. Findik, V.F. Smith, L.L. Randall, Penetration into membrane of amino-terminal region of SecA when associated with SecYEG in active complexes, Protein Sci. 27 (2018) 681–691, https://doi.org/10.1002/pro.3362.
[27] K. Nishiyama, M. Hanada, H. Tokuda, Disruption of the gene encoding p12 (SecG) reveals the direct involvement and important function of SecG in the protein translocation of Escherichia coli at low temperature, EMBO J. 13 (1994) 3272–3277.
[28] V.P. Kontinen, H. Tokuda, Overexpression of phosphatidylglycerophosphate synthase restores protein translocation in a secG deletion mutant of Escherichia coli at low temperature, FEBS Lett. 364 (1995) 157–160 (doi:001457939500378M [pii]).
[29] S. Das, D.B. Oliver, Mapping of the SecA.SecY and SecA.SecG interfaces by site-directed in vivo photocross-linking, Journal of Biological Chemistry. 286 (2011) 12371–12380. doi:https://doi.org/10.1074/jbc.M110.182931.
[30] R.A. Corey, E. Pyle, W.J. Allen, D.W. Watkins, M. Casiraghi, B. Miroux, I. Arechaga, A. Politis, I. Collinson, Specific cardiolipin–SecY interactions are required for proton-motive force stimulation of protein secretion, Proc. Natl. Acad. Sci. 201721536 (2018), https://doi.org/10.1073/pnas.1721536115.
[31] S. Kikuchi, I. Shibuya, K. Matsumoto, Viability of an Escherichia coli pgsA null mutant lacking detectable phosphatidylglycerol and cardiolipin viability of an Escherichia coli pgsA null mutant lacking detectable phosphatidylglycerol and cardiolipin, J. Bacteriol. 182 (2000) 371–376, https://doi.org/10.1128/JB.182.2.371-376.2000.Updated.
[32] J.H. Reithinger, C. Yim, S. Kim, H. Lee, H. Kim, Structural and functional profiling of the lateral gate of the sec61 translocon, J. Biol. Chem. 289 (2014) 15845–15855, https://doi.org/10.1074/jbc.M113.533794.
[33] G. von Heijne, Signal sequences. The limits of variation, J. Mol. Biol. 184 (1985) 99–105, https://doi.org/10.1016/0022-2836(85)90046-4.
[34] R.C.A. Keller, J.A. Killian, B. de Kruijff, Anionic phospholipids are essential for α-helix formation of the signal peptide of prephoe upon interaction with phospholipid vesicles, Biochemistry. 31 (1992) 1672–1677, https://doi.org/10.1021/bi00121a014.
[35] R.C.A. Keller, D. ten Berge, N. Nouwen, M.M.E. Snel, J. Tommassen, D. Marsh, B. de Kruijff, Mode of insertion of the signal sequence of a bacterial precursor protein into phospholipid bilayers as revealed by cysteine-based site-directed spectroscopy, Biochemistry. 35 (1996) 3063–3071, https://doi.org/10.1021/bi951870+.
[36] R.A. Demel, E. Goormaghtigh, B. de Kruijff, Lipid and peptide specificities in signal peptide-lipid interactions in model membranes, BBA-Biomembranes 1027 (1990) 155–162, https://doi.org/10.1016/0005-2736(90)90079-4.
[37] I. Prabudiansyah, I. Kusters, A.J.M. Driessen, In vitro interaction of the housekeeping SecA1 with the accessory SecA2 protein of *Mycobacterium tuberculosis*., PloS One. 10 (2015) doi: https://doi.org/10.1371/journal.pone.0128788. doi:https://doi.org/10.1371/journal.pone.0128788.
[38] D. Hanahan, Studies on transformation of Escherichia coli with plasmids, J. Mol. Biol. 166 (1983) 557–580, https://doi.org/10.1016/S0022-2836(83)80284-8.
[39] F. Baneyx, G. Georgiou, In vivo degradation of secreted fusion proteins by the Escherichia coli outer membrane protease OmpT, J. Bacteriol. 172 (1990) 491–494, https://doi.org/10.1128/jb.172.1.491-494.1990.
[40] F.W. Studier, B.A. Moffatt, Use of bacteriophage T7 RNA polymerase to direct selective high-level expression of cloned genes, J. Mol. Biol. 189 (1986) 113–130, https://doi.org/10.1016/0022-2836(86)90385-2.
[41] A. Kedrov, I. Kusters, V. V Krasnikov, A.J.M. Driessen, A single copy of SecYEG is sufficient for preprotein translocation., The EMBO Journal. 30 (2011) 4387–4397. doi:https://doi.org/10.1038/emboj.2011.314.
[42] J. de Keyzer, C. van der Does, A.J.M. Driessen, Kinetic analysis of the translocation of fluorescent precursor proteins into Escherichia coli membrane vesicles, J. Biol. Chem. 277 (2002) 46059–46065, https://doi.org/10.1074/jbc.M208449200.
[43] C. van der Does, J. de Keyzer, M. van der Laan, A.J.M. Driessen, Reconstitution of purified bacterial preprotein translocase in liposomes, Methods Enzymol. 372 (2003) 86–98, https://doi.org/10.1016/S0076-6879(03)72005-9.
[44] O.D. Bello, S.M. Auclair, J.E. Rothman, S.S. Krishnakumar, Using ApoE-nanolipoprotein particles to analyze SNARE-induced fusion pores, Langmuir. 32 (2016) 3015–3023, https://doi.org/10.1021/acs.langmuir.6b00245.
[45] M. van der Laan, E.N. Houben, N. Nouwen, J. Luirink, A.J.M. Driessen, Reconstitution of Sec-dependent membrane protein insertion: nascent FtsQ interacts with YidC in a SecYEG-dependent manner, EMBO Rep. 2 (2001) 519–523, https://doi.org/10.1093/embo-reports/kve106.
[46] R. Bol, J.G. de Wit, A.J.M. Driessen, The active protein-conducting channel of Escherichia coli contains an apolar patch, J. Biol. Chem. 282 (2007) 29785–29793, https://doi.org/10.1074/jbc.M702140200.
[47] S. Jain, A. Caforio, P. Fodran, J.S. Lolkema, A.J. Minnaard, A.J.M. Driessen, Identification of CDP-Archaeol synthase, a missing link of ether lipid biosynthesis in archaea, Chem. Biol. 21 (2014) 1392–1401, https://doi.org/10.1016/j.chembiol.2014.07.022.
[48] M.J. Abraham, T. Murtola, R. Schulz, S. Páll, J.C. Smith, B. Hess, E. Lindah, Gromacs: high performance molecular simulations through multi-level parallelism from laptops to supercomputers, SoftwareX. 1–2 (2015) 19–25, https://doi.org/10.1016/j.softx.2015.06.001.
[49] D.H. de Jong, G. Singh, W.F.D. Bennett, C. Arnarez, T.A. Wassenaar, L.V. Schäfer, X. Periole, D.P. Tieleman, S.J. Marrink, Improved parameters for the martini coarse-grained protein force field, J. Chem. Theory Comput. 9 (2013) 687–697, https://doi.org/10.1021/ct300646g.
[50] T.A. Wassenaar, H.I. Ingólfsson, R.A. Böckmann, D.P. Tieleman, S.J. Marrink, Computational lipidomics with insane: a versatile tool for generating custom membranes for molecular simulations, J. Chem. Theory Comput. 11 (2015) 2144–2155, https://doi.org/10.1021/acs.jctc.5b00209.
[51] X. Periole, M. Cavalli, S.J. Marrink, M.A. Ceruso, Combining an elastic network with a coarse-grained molecular force field: structure, dynamics, and intermolecular recognition, J. Chem. Theory Comput. 5 (2009) 2531–2543, https://doi.org/10.1021/ct9002114.
[52] D.H. de Jong, S. Baoukina, H.I. Ingólfsson, S.J. Marrink, Martini straight: boosting performance using a shorter cutoff and GPUs, Comput. Phys. Commun. 199 (2016) 1–7, https://doi.org/10.1016/j.cpc.2015.09.014.
[53] T.A. Wassenaar, K. Pluhackova, R.A. Böckmann, S.J. Marrink, D.P. Tieleman, Going backward: a flexible geometric approach to reverse transformation from coarse grained to atomistic models, J. Chem. Theory Comput. 10 (2014) 676–690, https://doi.org/10.1021/ct400617g.
[54] J. Huang, A.D. Mackerell, CHARMM36 all-atom additive protein force field: validation based on comparison to NMR data, J. Comput. Chem. 34 (2013) 2135–2145, https://doi.org/10.1002/jcc.23354.
[55] W.L. Jorgensen, J. Chandrasekhar, J.D. Madura, R.W. Impey, M.L. Klein, Comparison of simple potential functions for simulating liquid water, J. Chem. Phys. 79 (1983) 926–935, https://doi.org/10.1063/1.445869.
[56] A.D. MacKerell, D. Bashford, M. Bellott, R.L. Dunbrack, J.D. Evanseck, M.J. Field, S. Fischer, J. Gao, H. Guo, S. Ha, D. Joseph-McCarthy, L. Kuchnir, K. Kuczera, F.T. Lau, C. Mattos, S. Michnick, T. Ngo, D.T. Nguyen, B. Prodhom, W.E. Reiher, B. Roux, M. Schlenkrich, J.C. Smith, R. Stote, J. Straub, M. Watanabe, J. Wiorkiewicz-Kuczera, D. Yin, M. Karplus, All-atom empirical potential for molecular modeling and dynamics studies of proteins., The Journal of Physical Chemistry. B. 102 (1998) 3586–3616. doi:https://doi.org/10.1021/jp973084f.
[57] S. Miyamoto, P.A. Kollman, Settle: an analytical version of the SHAKE and RATTLE algorithm for rigid water models, J. Comput. Chem. 13 (1992) 952–962, https://doi.org/10.1002/jcc.540130805.
[58] B. Hess, P-LINCS: a parallel linear constraint solver for molecular simulation., Journal of Chemical Theory and Computation. 4 (2008) 116–122. doi:https://doi.org/10.1021/ct700200b.
[59] T. Darden, D. York, L. Pedersen, Particle mesh Ewald: an N·log(N) method for Ewald sums in large systems, J. Chem. Phys. 98 (1993) 10089–10092, https://doi.org/10.1063/1.464397.
[60] M. Parrinello, A. Rahman, Polymorphic transitions in single crystals: a new molecular dynamics method, J. Appl. Phys. 52 (1981) 7182–7190, https://doi.org/10.1063/1.328693.
[61] G. Bussi, D. Donadio, M. Parrinello, Canonical sampling through velocity rescaling, J. Chem. Phys. 126 (2007) 14101, https://doi.org/10.1063/1.2408420.